Future Integrative Medicine **2024** vol. 3(2) | 75–86
DOI: 10.14218/FIM.2024.00005

Original Article

Transcriptomics-based Study on the Mechanism of Heart Failure Amelioration by Water Decoction and Water-soluble Alkaloids of Fuzi

Jing Zhang[1#], Dan Zhong[2#], Feixia Hou[1], Xiaofang Xie[1], Jihai Gao[1*] and Cheng Peng[1*]

[1]*State Key Laboratory of Southwestern Chinese Medicine Resources, School of Pharmacy, Chengdu University of Traditional Chinese Medicine, Chengdu, Sichuan, China;* [2]*Hospital of Chengdu University of Traditional Chinese Medicine, Chengdu, Sichuan, China*

Received: February 21, 2024 | **Revised:** May 06, 2024 | **Accepted:** May 11, 2024 | **Published online:** June 28, 2024

Abstract

Background and objectives: Fuzi, the processed product of daughter roots of *Aconitum carmichaelii* Debx., is a well-known Chinese medicine for the treatment of heart failure (HF) and related cardiac diseases. This study aimed to investigate the molecular mechanism of the cardioprotective effects of Fuzi water decoction (FWD) and Fuzi water-soluble alkaloids (FWA) on the model of HF.

Methods: The HF model of rats was prepared through intravenous injection of propafenone hydrochloride. The normal group, model group, FWD-treated groups (1.25 g/kg, 2.5 g/kg, 5 g/kg) and positive group (Shenfu Injection, 3.3 mL/kg) were set up. Heart rate, LV+dp/dt$_{max}$, and LV-dp/dt$_{max}$ were recorded at 5 m, 10 m, 20 m, 30 m, and 60 m after drug administration, respectively. The contents of atrial natriuretic peptide, brain natriuretic peptide (BNP), angiotensin II, and aldosterone in serum were determined 20 m post-administration. An *in vitro* cardiomyocyte hypertrophy model with *HDAC2* overexpression was constructed and verified by lentivirus transfection. The experiment included a blank group, FWD-treated groups (3 mg/mL, 1.5 mg/mL), and FWA-treated groups (4 mg/mL, 2 mg/mL). For transcriptome analysis, the model group, blank group, and FWD-treated group (2.5 g/kg) at 20 m and 60 m *in vivo*, and different dose groups *in vitro*, were selected to analyze the therapeutic mechanisms of FWD and FWA.

Results: All FWD treatment groups showed an increased heart rate, among which the groups with 2.5 g/kg and 5 g/kg FWD showed better effects, significantly increasing LV+dp/dt$_{max}$ and LV-dp/dt$_{max}$ after 20 m of administration and significantly reducing BNP and aldosterone serum levels. In the constructed cardiomyocyte hypertrophy model, *HDAC2* expression, atrial natriuretic peptide and BNP protein levels, and cell surface area increased. Transcriptome data from both *in vivo* and *in vitro* showed that FWD and FWA could exert cardioprotective effects through pathways such as the PI3K-Akt signaling pathway, NF-κB signaling pathway, and ATP-binding cassette (ABC) transporters, involving key genes such as *ITGB1*, *TLR2*, and *CDKN1A*. Fuzi inhibited the hypertrophic gene *HDAC2*. Additionally, based on weighted gene co-expression network analysis, ABC transporters may be an important molecular pathway for FWA in treating HF.

Conclusions: Both FWD and FWA can ameliorate HF by regulating apoptosis, proliferation, and anti-fibrosis, with ABC transporters potentially being the main pathway for the action of FWA.

Keywords: Fuzi; Heart failure; *HDAC2*; Cardiac hypertrophy; Lentiviral; ABC transporters.

[*]**Correspondence to:** Jihai Gao and Cheng Peng, State Key Laboratory of Southwestern Chinese Medicine Resources, School of Pharmacy, Chengdu University of Traditional Chinese Medicine, Chengdu, Sichuan 611137, China. ORCID: https://orcid.org/0000-0002-5153-821X (JHG); https://orcid.org/0000-0003-3303-906X (CP). Tel: +86-28-61800231 (JHG); +86-13708237099 (CP), E-mail: gaojihai@cdutcm.edu.cn (JHG); peng_cutcm@126.com (CP)

[#]These authors contributed equally to this work.

How to cite this article: Zhang J, Zhong D, Hou F, Xie X, Gao J, Peng C. Transcriptomics-based Study on the Mechanism of Heart Failure Amelioration by Water Decoction and Water-soluble Alkaloids of Fuzi. *Future Integr Med* 2024;3(2):75–86. doi: 10.14218/FIM.2024.00005.

Introduction

Heart failure (HF), one of the major diseases that pose serious threats to human health, affects about 40 million people worldwide.[1] The pathogenesis of HF is diverse and closely associated with dynamic interactions between ventricular remodeling, in-

creased hemodynamic load, and excessive neurohumoral stimulation.[2] While HF has traditionally been thought of as a disease of the elderly, new research suggests that the number of younger patients being hospitalized for HF is rising at an alarming rate.[3] HF is treated with a variety of therapies, such as interventions including medications, diet, and medical devices, but a large percentage of people still struggle to live a healthy life.[4] In Western countries, the mortality rate for HF patients is even close to 50%.[5]

HDAC2, a class I member of the HDAC superfamily, is thought to be pro-hypertrophic and harmful in HF.[6,7] Furthermore, cardiomyocyte-specific overexpression of *HDAC2* leads to severe cardiac hypertrophy.[6] Cardiac hypertrophy is a pathophysiological process in various cardiovascular diseases characterized by increased protein synthesis, increased size, cardiomyocyte fibrosis, and increased interstitial components; however, persistent cardiac hypertrophy can lead to HF.[5]

Fuzi, the processed product of daughter roots of *Aconitum carmichaelii* Debx., was first recorded in *Shennong's Classic of Materia Medica*. It has shown efficacy in reviving the *Yang* for resuscitation, tonifying fire, helping *Yang*, as well as dispersing cold and relieving pain.[8] It is commonly used for the treatment of HF,[9,10] rheumatoid arthritis,[11,12] and various types of pain, and is widely used in Asian countries. For example, common clinical pairs like Fuzi-*Zingiberis* Rhizoma and Fuzi-*Ginseng* Radix et Rhizoma have shown cardioprotective effects.[13,14] And Qiliqiangxin capsules and Shenfu Injection are classic herbal combinations for the treatment of HF in China.[15,16] In addition, total and water-soluble alkaloids of Fuzi have been shown to have cardiotonic effects on the failing heart.[17]

The chemical composition of Fuzi is diverse, with relatively thorough research on liposoluble alkaloids. Current studies have shown that the Fuzi water-soluble alkaloids (FWA) possess significant cardiotonic and anti-inflammatory effects. However, due to their low content and limited known components, research on their pharmacological mechanisms is still insufficient.[18] Therefore, further research on FWA will help deeply analyze the molecular mechanism of its cardiotonic effect. This study utilized propafenone hydrochloride to construct an animal model of HF *in vivo*, avoiding the severe cardiac toxicity and liver-kidney dysfunction caused by doxorubicin-induced HF.[19] Additionally, lentiviral vectors were used to construct cardiomyocytes overexpressing *HDAC2*, and the molecular mechanisms of FWD and FWA in treating HF were explored from the perspective of transcriptomics.

Materials and methods

Preparation of FWD and FWA

FWD and FWA were provided by the State Key Laboratory of Southwest Chinese Medicine Resources, Chengdu University of Traditional Chinese Medicine. One milliliter of FWD corresponded to 1.086 g of raw Fuzi, and the HPLC (high performance liquid chromatography) assay method determined that each gram of FWD contained 2.918 μg of benzoylaconitine, 1.129 μg of aconitine, and 0.161 μg of benzoylmesaconine. Mesaconitine, hypaconitine, and benzoylhypaconitine were not detected. The yield of FWA from Fuzi was 8.4% (W/W), and the detected levels of aconine, hypaconine, fuziline, neoline, talatisamine, and songrine were 0.060%, 0.200%, 0.210%, 0.510%, 0.010%, and 0.004%, respectively.[20]

Experimental animals and protocols

Sprague-Dawley rats (250 ± 20 g, approval No. SCXK 2017-11) of mixed gender were supplied by the Animal Center of Chengdu University of Traditional Chinese Medicine (Sichuan, China). The animal care adhered to the Guidelines for Animal Experimentation of Chengdu University of TCM, and the protocol was approved by the Animal Ethics Committee of the institution (ethics number: 2023020). After one week of adaptive feeding, all rats were randomly divided into six groups (n = 8): blank group (KB), model group (M), low-dose group (1.25 g/kg, D), middle-dose group (2.5 g/kg, Z), high-dose group (5 g/kg, G) of the FWD, and the positive group (Y) treated with 3.3 mL/kg of Shenfu Injection. An HF rat model was created using 16.5 mg/kg propafenone hydrochloride injection into the femoral vein. Distilled water was given to the model group, a tail vein injection was administered to the positive group, and duodenal administration was given to all dose groups. Heart rate, the maximum rate of increase in left ventricular pressure ($LV+dp/dt_{max}$), and the maximum rate of decrease in left ventricular pressure ($LV-dp/dt_{max}$) were recorded at 5 m, 10 m, 20 m, 30 m, and 60 m after drug administration. Another batch of rats was modeled and administered in the same way, and blood samples were collected 20 m after administration. The contents of atrial natriuretic peptide (ANP), brain natriuretic peptide (BNP), angiotensin II (Ang-II), and aldosterone (ALD) in serum were detected using ELISA (enzyme-linked immunosorbent assay) kits.

Construction and validation of a cellular model of cardiac hypertrophy

The H9C2 cells and 293T cells were purchased from Chongqing Biomedicine Biotechnology Co., Ltd (Chongqing, China). All cells were cultured in a medium (90% dulbecco's modified eagle medium, 10% fetal bovine serum, 100 U/mL of penicillin, 100 mg/mL of streptomycin) and in a humidified atmosphere containing 5% CO_2 at 37°C. The *HDAC2* sequence (Gene ID: NM_053447, 1467bp) was obtained through gene synthesis (forward primer: 5′-ATGGCGTACAGTCAAGGAGG-3′; reverse primer: 5′-TCAAGGGTTGTTGAGTTGTTC-3′) and constructed into the lentiviral vector pLVX-TetOne-Puro-HDAC2 (Chongqing Biomedicine Biotechnology Co., Ltd, Chongqing, China). The *HDAC2* in the lentiviral expression vector was controlled by the TRE3GS promoter, followed by the gene for enhanced green fluorescent protein (GFP). The resulting vector plasmid, pLVX-TetOne-Puro-HDAC2, was used to generate recombinant lentiviral particles, and the lentiviral vector expressing only GFP was used as a negative control (NC). The recombinant lentiviral pLVX-TetOne-Puro-HDAC2 was cotransfected into 293T cells with plasmids pMD2.G and psPAX2, and the packaged recombinant lentivirus was collected by centrifugation. H9C2 cells in the logarithmic growth phase were divided into the NC group, control group, and overexpressing HDAC2 group. Spread to 12-well plates at 1×10^5 cells/well, when the cells reached about 2×10^5 cells/well, the medium was replaced with fresh medium, and 30 μL of pLVX-TetOne-Puro lentiviral vector, pLVX-TetOne-Puro-HDAC2, and 5 μg/mL of polybrene were added to the NC group and overexpression group, respectively. After 48 h of incubation, the cells were replaced with a fresh complete culture medium containing 5 μg/mL puromycin and screened until the virus fully infected the cells, during which the cell status was observed using fluorescence microscopy. H9C2 cells were transfected for 24 h and 36 h later, and the relative expression of *HDAC2* in each group was verified using quantitative real-time polymerase chain reaction (qRT-PCR). The primer sequences are listed in Table 1. Western blot was used to detect ANP and BNP content in each group of cellular proteins. After transfection, cell images under 100x magnification were cap-

Table 1. qRT-PCR primer sequences

Gene	Forward (5′-3′)	Reverse (5′-3′)
HDAC2	AGACTGCAGTTGCCCTTGAT	CAGGCGCATGTGGTAACATT
GAPDH	GCAAGTTCAACGGCACAG	GCCAGTAGACTCCACGACATA-

GAPDH, glyceraldehyde-3-phosphate dehydrogenase; *HDAC2*, histone deacetylase 2; qRT-PCR, quantitative real-time polymerase chain reaction.

tured using an inverted microscope. Ten fields of view were randomly selected for each group, and the surface area of the cells in each group was measured using Image-Pro Plus 6.0 software and averaged. At least 50 cells were analyzed in each group.

Cell culture

Well-grown pLVX-HDAC2 H9C2 cardiomyocytes were spread into 6-well plates at 3×10^5 cells/well and divided into blank and drug-dosing groups, with three biological replicates in each group. The blank group was given 1% serum medium, and drug-dosing groups were given Fuzi water decoction - high dose (FWDG) (3 mg/mL), Fuzi water decoction - low dose (FWDD) (1.5 mg/mL), Fuzi water-soluble alkaloids - high dose (FWAG) (4 mg/mL), and Fuzi water-soluble alkaloids - low dose (FWAD) (2 mg/mL) respectively.

RNA extraction, next-generation sequencing, and bioinformatics analysis

Two rats from each of the blank control group, model group, and FWD medium-dose group were selected and given drugs for 20 m and 60 m, respectively. At the end of the treatment, the rats were sacrificed, and their hearts were carefully excised and rapidly frozen in liquid nitrogen. In the *in vitro* cell experiments, the cells need to be cultured for 24 h after drug administration. Total RNA was extracted using the RaPure total RNA Mini Kit. NanoDrop™ and Qubit™ 4.0 fluorometers were used to assess RNA quality. The complementary DNA library was constructed and sequenced using the Illumina NovaSeq 6000 platform. After filtering out low-quality data from the raw data, clean reads were obtained, and transcript sequences were assembled. The DEGseq software was used to analyze the differentially expressed genes between groups, resulting in a set of differentially expressed genes. Based on FPKM (fragments per kilobase of exon model per million mapped fragments) expression analysis, the screening criteria were set as FDR (False Discovery Rate) <0.01 and FC (fold change) ≥2. Enrichment analysis was performed on the differentially expressed genes annotated in the gene ontology (GO) and Kyoto encyclopedia of genes and genomes (KEGG) databases, and the weighted gene co-expression network analysis (WGCNA) toolkit was used to construct co-expression modules.

qRT-PCR

Based on the transcriptome sequencing results, five differentially expressed genes were randomly selected, and messenger RNA (mRNA) levels were determined using real-time PCR with glyceraldehyde-3-phosphate dehydrogenase as the internal reference gene. The PCR primers were designed using Primer5 (Table 2), and the experiment was repeated three times for each gene.

Statistical analysis

All data were presented as means ± SD and analyzed with GraphPad Prism 8.2.1 software (San Diego, CA, USA). Comparisons of means between groups were analyzed using one-way ANOVA. Multiple comparisons were performed using the *LSD-t* test. Differences were indicated as statistically significant at $p < 0.05$.

Results

Protective effect of FWD on rats with HF

To detect the therapeutic effects of FWD on rats with HF, we measured heart rate, LV+dp/dt_{max}, and LV-dp/dt_{max}. The results showed that all dose groups of the FWD decoction improved heart rate compared with the model group, especially in the Z group (2.5 g/kg) and G group (5 g/kg) during the period of 10–60 m of administration (Fig. 1a). There was a significant difference in the effect of each dose group on LV+dp/dt_{max} from 20–60 m of administration (Fig. 1b), and the effect on LV-dp/dt_{max} was significantly different from 10–60 m of administration in all cases (Fig. 1c). Additionally, serum levels of ANP, BNP, ALD, and Ang-II were elevated in rats after modeling, while BNP and ALD levels were significantly reduced in the Z group and G group of FWD after administration for 20 m (Fig. 1d).

Transcriptome sequencing and analysis of rat heart tissue

Based on the above protective effect of the FWD decoction on rats with HF, the middle dose group (2.5 g/kg) was selected as the experimental group by administering the drug for 20 m and 60 m (Z20, Z60). A total of eight samples from the KB group, the M group, and the experimental group were included for transcriptome analysis.

Overall, 173 genes were up-regulated, and 132 genes were down-regulated in the M group compared with the KB group (Fig. 2a). In the Z20 group, 98 genes were up-regulated and 143 genes were down-regulated compared to the M group (Fig. 2b), with a significant increase in up-regulated genes in the Z60 group, total-

Table 2. Primer sequences used for quantitative polymerase chain reaction

Gene	Forward (5′-3′)	Reverse (5′-3′)
ITGA11	GCAGTGACAGTAATGAGCGG	TGAAGATGCAGCTGAAGGGA
Rrm2	ACTGTGACTTTGCCTGCCTGATG	TCCGTGAGGAACTCCTGCTCTATC
SLC7A5	CATCATCGGTTCGGGCATCT	CCGCCTGACTTTGAGATGGT
IL23	ATAAGCACCTGCTGGACTCG	GGAACGGAGAAGAGAACGCT
LAMTOR	CAGTGCTAGCGTCATCTGGG	GCAGCGTGTGTTCACCAAAG

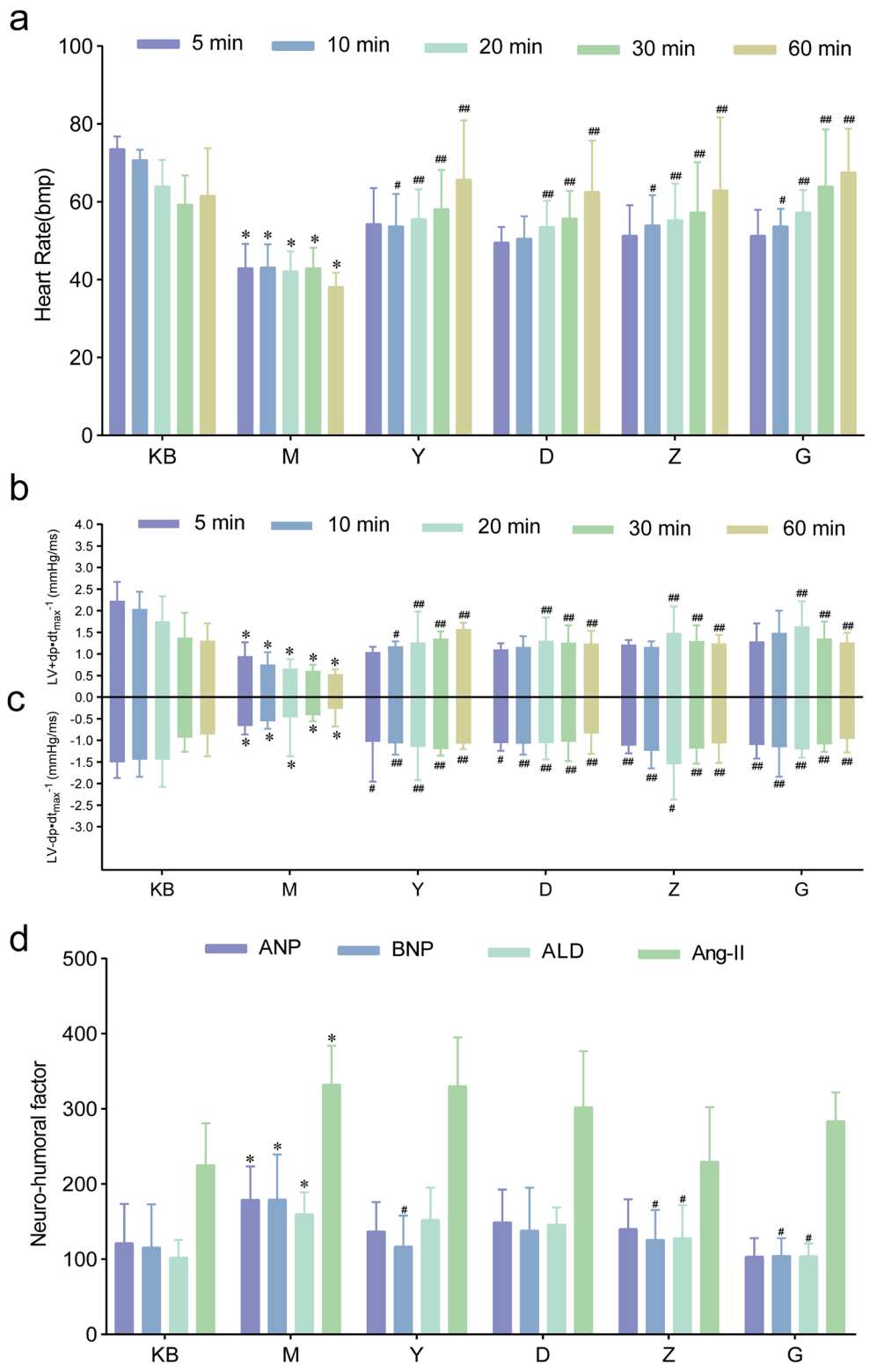

Fig. 1. FWD improved heart function in propafenone hydrochloride-induced rats. (a) The change of heart rate; (b) The change of LV+dp/dt_{max}; (c) The change of LV-dp/dt_{max}; (d) Serum levels of neuro-humoral factors (n = 8, $^{*}p < 0.05$ vs. the KB group; $^{\#}p < 0.05$ and $^{\#\#}p < 0.01$ vs. the M group). ALD, aldosterone; Ang-II, angiotensin II; ANP, atrial natriuretic peptide; BNP, brain natriuretic peptide; D, low-dose group; FWD, Fuzi water decoction; G, high-dose group; KB, blank group; LV+dp/dt_{max}, the maximal rising rate of left ventricle pressure; LV-dp/$dt_{max,}$ the maximal declining rate of left ventricle pressure; M, model group; Y, positive group; Z, middle-dose group.

 DOI: 10.14218/FIM.2024.00005 | Volume 3 Issue 2, June 2024

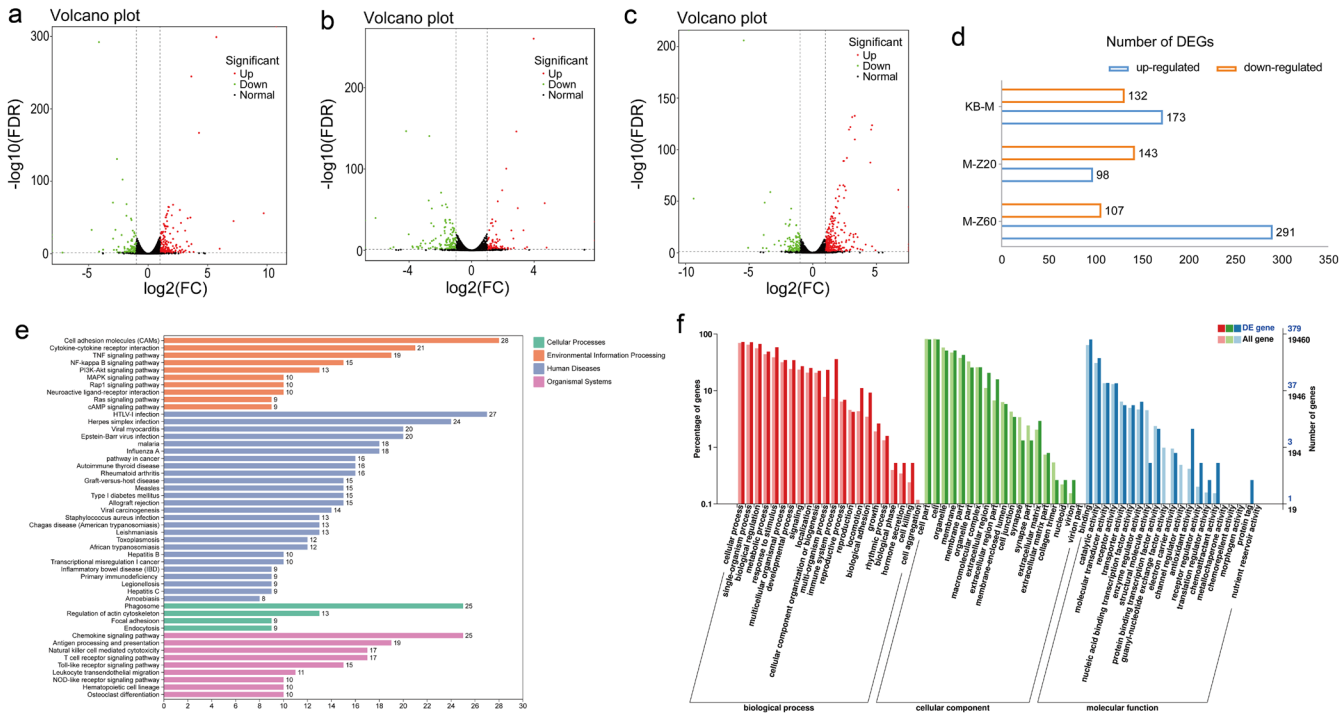

Fig. 2. Transcriptomic assay and bioinformatics analysis of rat heart by FWD. (a) Difference expression volcano map between KB-M groups; (b) Difference expression volcano map between M-Z20 groups; (c) Difference expression volcano map between M-Z60 groups; (d) Integration map of DEGs; (e) KEGG enrichment and classification of DEGs in M group and Z60 group; (f) GO classification of DEGs in M group and Z60 group. DEGs, differential expression genes; FWD, Fuzi water decoction; GO, gene ontology; KB, blank group; KEGG, Kyoto encyclopedia of genes and genomes; M, model group; Z20, Administer Fuzi water decoction-mild dose for 20 minutes; Z60, Administer Fuzi water decoction-mild dose for 60 minutes.

ing 291 genes, while 107 genes were down-regulated (Fig. 2c).

To further explore the potential mechanism of FWD in treating HF, we performed a KEGG metabolic pathway enrichment analysis of the differential genes. The results showed that 202 differential genes were annotated to the KEGG metabolic pathway in the Z60 group compared with the model group after 60 m of administration (Fig. 2b). Among these, the tumor necrosis factor (TNF) signaling pathway, nuclear factor Kappa-B (NF-κB) signaling pathway, and phosphatidylinositol-3-kinase-Akt (PI3K-Akt) signaling pathway were the most important enriched signaling pathways. Additionally, GO pathway annotation enrichment analysis of differential genes revealed that the cellular process was the most significantly enriched pathway in biological processes. For cellular component enrichment analysis, differential expression genes (DEGs) were mainly enriched in the “cell part”, “cell” and other pathways. Moreover, “binding” was the most obvious pathway for molecular function (Fig. 2c).

Cell model validation

The *HDAC2* mRNA sequence was successfully cloned into the pLVX-TetOne-Puro (Fig. 3a), and the recombinant lentiviral vector was verified by DNA sequencing, confirming the correct insertion of the cloned *HDAC2* sequence. GFP protein expression in recombinant lentivirus-transfected target cells was observed using fluorescence microscopy, showing green fluorescence in the NC and pLVX-HDAC2 groups, but not in the control group (Fig. 3b). Compared to the NC group, *HDAC2* mRNA expression was significantly higher in the pLVX-HDAC2 group, both at 24 h and 36 h (**$p < 0.01$, Fig. 3c), with a corresponding increase in HDAC2 protein (*$p < 0.05$, Fig. 3d). These results indicate successful expression and translation of exogenous *HDAC2* in H9C2 cells of the pLVX-HDAC2 group. Additionally, there was a significant increase in cell surface area and expression of ANP and BNP proteins in the pLVX-HDAC2 group cells (*$p < 0.05$, Fig. 3e, f).[21]

Cell model transcriptome sequencing analysis

A total of 13 samples from five groups, KB (pLVX-HDAC2), FWDD, FWDG, FWAG, and FWAG, were sequenced. Differential genes were all higher in the high-dose group compared to the KB group, and the number of DEGs was higher in FWAG. For instance, compared to the KB group, the FWDG group had 1338 DEGs, with 1284 up-regulated genes and 54 down-regulated genes, while the FWAG group had 1980 DEGs, including 1630 up-regulated genes and 350 down-regulated genes. Among the differentially expressed genes between the FWD and FWA groups, there were 269 up-regulated and 207 down-regulated genes (Fig. 4a).

Regarding the *HDAC2* gene, we observed down-regulation in both the FWD and FWA groups, along with down-regulation of genes associated with *HDAC2*, such as *HSP70*, *FOXO3a*, *mTOR*, and *CDKN1A* (Fig. 4b). We further explored the biological pathways involved in cardiac hypertrophy by FWD and FWA through KEGG metabolic pathway (Fig. 4c, 4d). Compared to the KB group, the up-regulated differential genes in both FWDG and FWAG were significantly enriched in the ATP-binding cassette (ABC) transporter and PI3K-Akt signaling pathway, etc., while the FWDG group down-regulated the expression of genes in the signaling pathways such as the HIF-1 signaling pathway, Rap1 signaling pathway, NF-κB signaling pathway, p53 signaling

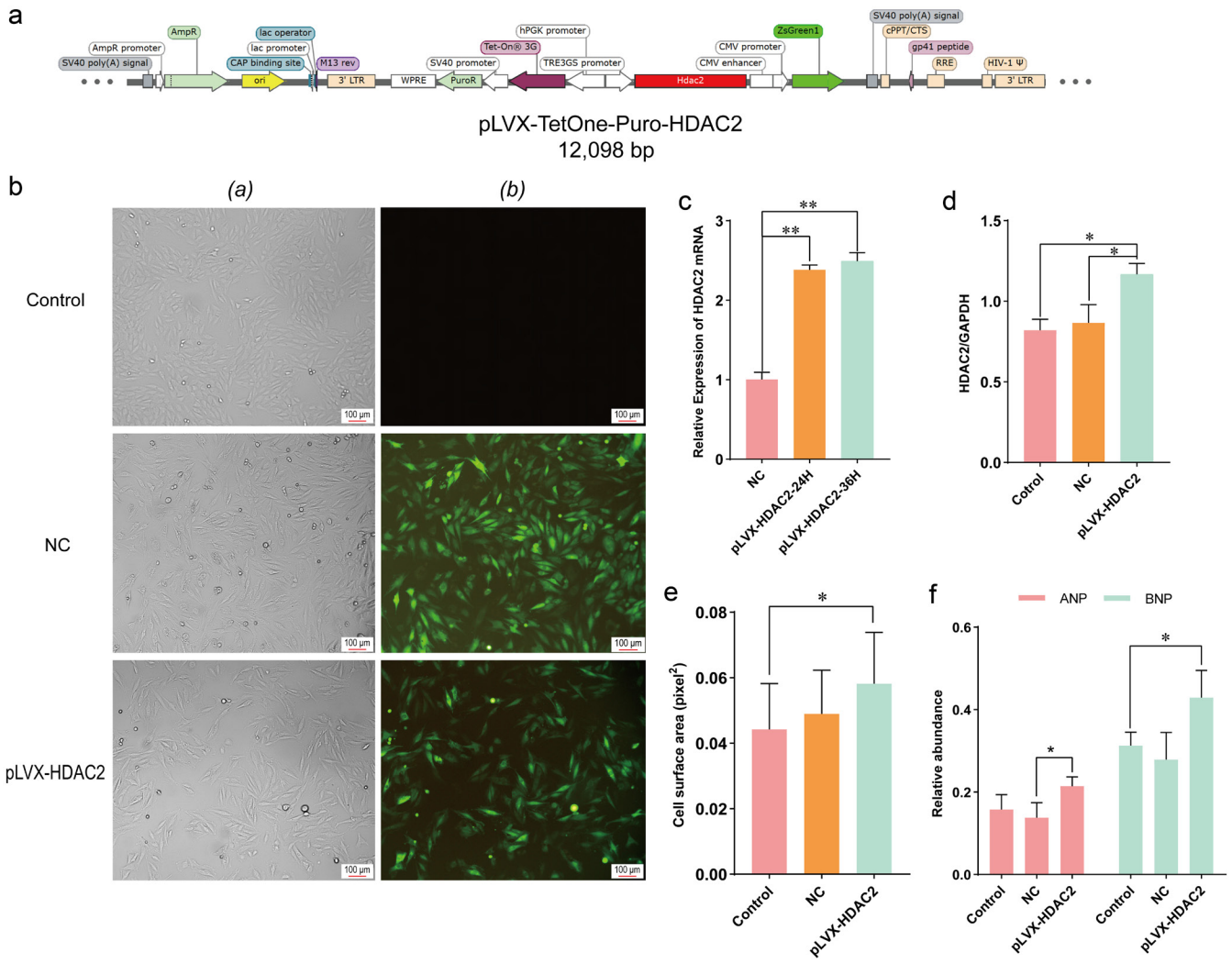

Fig. 3. Validation of indicators of cardiac hypertrophy cell model. (a) Genetic structure of the lentiviral vector. Cartoon representing the genetic structure of the HIV-1-derived lentiviral vector. The red pattern represents the inserted target gene, ZsGreen1, *Zoanthus sp*. Green fluorescent protein; (b) Observation of green fluorescence in the control group, NC group, and pLVX-HDAC2 group, a is the field of view under bright field and b is the field of view under fluorescence; (c) The relative expression of *HDAC2* mRNA in NC group and pLVX-HDAC2 group; (d) HDAC2 protein content in the control group, NC group, and pLVX-HDAC2 group; (e) Cell surface area of the control group, NC group and pLVX-HDAC2 group; (f) ANP and BNP protein content in control group, NC group and pLVX-HDAC2 group. ANP, atrial natriuretic peptide; BNP, brain natriuretic peptide; CAP, catabolite gene activator protein; CMV, cytomegalovirus; cPPT, central polypurine tract; CTS, Chain termination sequence; HIV-1, human immunodeficiency virus-1; NC, negative control; pLVX-HDAC2, pLVX - histone deacetylase 2; RRE, rev response element; WPRE, the woodchuck hepatitis virus post-transcriptional response element.

pathway, Ras signaling pathway, mitogen-activated protein kinase (MAPK) signaling pathway, Wnt signaling pathway, mTOR signaling pathway, Calcium signaling pathway, and Janus kinase-signal transducer and activator of transcription (JAK-STAT) signaling pathway. FWAG down-regulated differential genes were significantly enriched in the JAK-STAT signaling pathway, NF-κB signaling pathway, MAPK signaling pathway, Calcium signaling pathway, and mTOR signaling pathway. Based on the above pathways of differential gene enrichment, we identified several key differential genes involved in the pathologic development of HF (Table 3).

Based on WGCNA, a total of 1820 genes were expressed in both the FWD group and FWA group, yielding two co-expression modules that showed a positive correlation with the FWD group (blue, r = 0.91, p = 0.03) and the FWA group (turquoise, r = 0.75, p = 0.1) (Fig. 5a, b). We conducted a KEGG enrichment analysis of genes from both modules. In the blue module, genes were significantly enriched in the Hippo signaling pathway, PI3K-Akt signaling pathway, Rap1 signaling pathway, cytokine-cytokine receptor interactions, and extracellular matrix (ECM)-receptor interactions (Fig. 5c). In the turquoise module, genes were significantly enriched in ABC transporters, aminoacyl-tRNA biosynthesis, ribosomes, and biosynthesis of amino acids (Fig. 5d).

RNA sequencing validation

To validate the results obtained from RNA sequencing analysis, we randomly selected five differential genes for qRT-PCR validation (Fig. 6). The results showed that FWD reduced the expres-

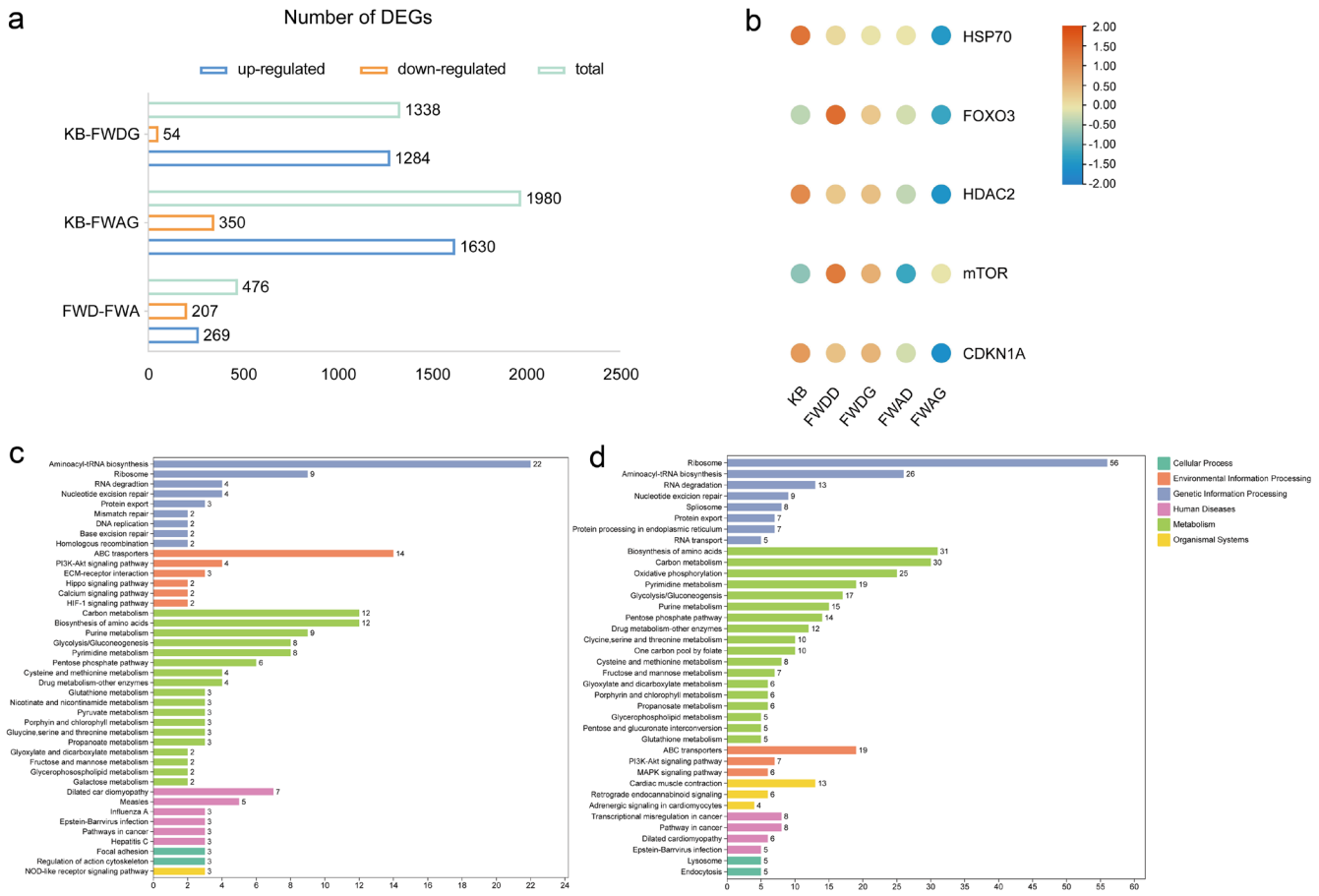

Fig. 4. Transcriptomic assay and bioinformatics analysis of cardiac hypertrophy cells by FWD and FWA. (a) Integration map of DEGs; (b) Heat maps of *HSP70*, *FOXO3a*, *mTOR*, and *CDKN1A*; (c) KEGG enrichment and classification of differentially expressed genes in KB group and FWDG group;(d) KEGG enrichment and classification of differentially expressed genes in KB group and FWAG group. DEGs, differential expression genes; FWA, Fuzi water-soluble alkaloids; FWAD, Fuzi water-soluble alkaloids - low dose; FWAG, Fuzi water-soluble alkaloids - high dose; FWD, Fuzi water decoction; FWDD, Fuzi water decoction - low dose; FWDG, Fuzi water decoction - high dose; KB, blank group; KEGG, Kyoto encyclopedia of genes and genomes.

sion of *ITGA11* and increased the expression of *Rrm2*, and the administration of different doses of FWD and FWA decreased the expression of *SCL7A5*, *IL23*, and *LAMTOR*, which was consistent with the trend of results obtained from RNA sequencing analysis. The current results suggest that both FWD and FWA are effective in alleviating certain indices in *ex vivo* and *in vivo*

Table 3. The key differential genes in transcriptome data

Gene name	Pathway ID	Log_2FC	Regulated
ITGB1	PI3K-Akt signaling pathway	1.23	up
Abcb7	ABC transporters	1.92	up
Abcc8	ABC transporters	3.69	up
Abcb10	ABC transporters	2.78	up
ITGA8	PI3K-Akt signaling pathway	1.68	up
TLR2	PI3K-Akt signaling pathway	−1.08	down
MYC	MAPK signaling pathway, PI3K-Akt signaling pathway	−1.45	down
SLC7A5	mTOR signaling pathway	−1.50	down
PKA	Ras signaling pathway	−1.13	down
CDKN1A	p53 signaling pathway	−2.71	down

ABC, ATP-binding cassette; MAPK, mitogen-activated protein kinase; mTOR, mammalian target of rapamycin; PI3K-Akt, phosphatidylinositol-3-kinase-Akt.

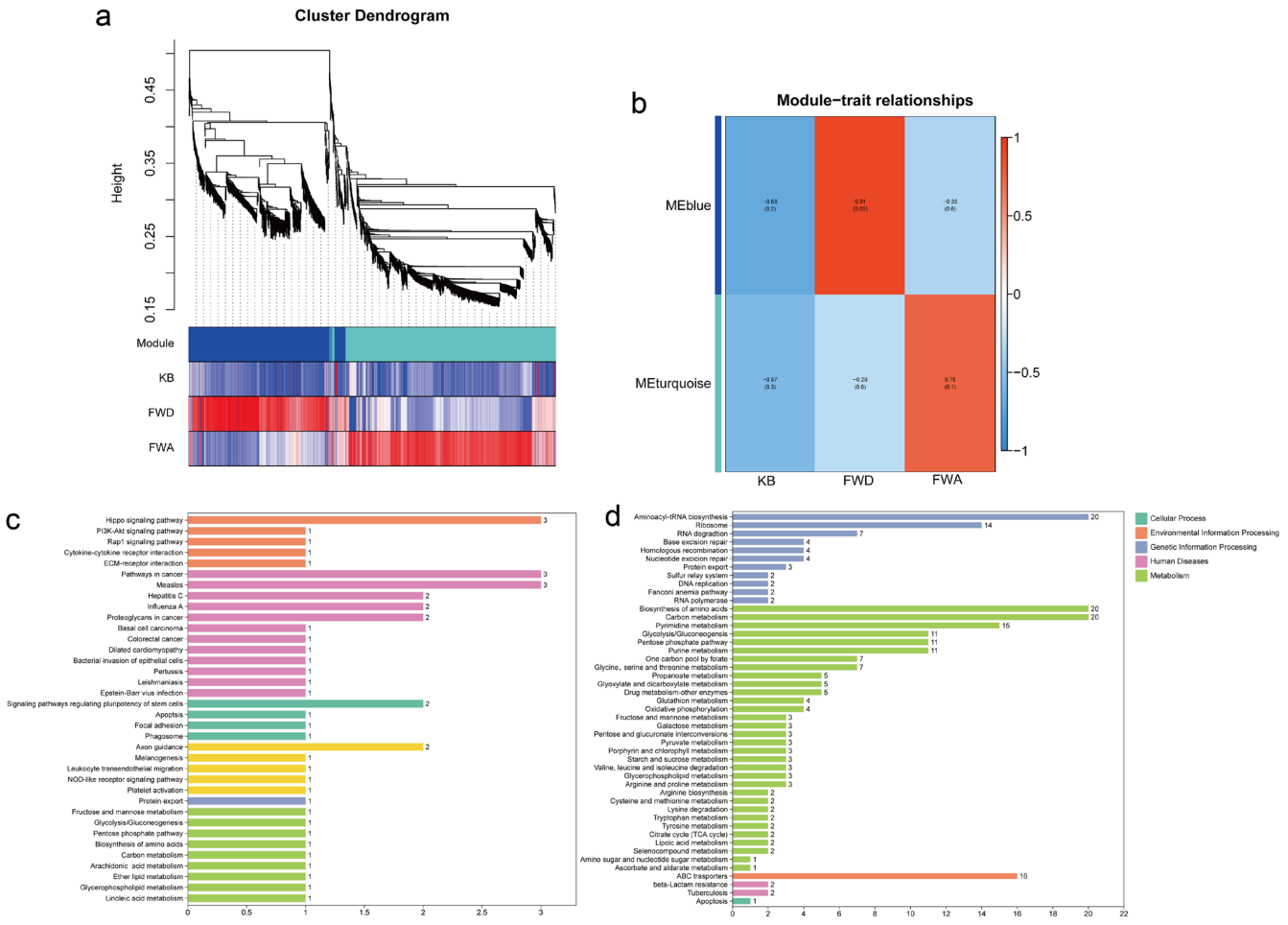

Fig. 5. The co-expression modules analysis. (a) Clustering dendrogram of genes; (b) The relationships of two modules and three traits; (c) KEGG enrichment analysis of functional genes in the blue module; (d) KEGG enrichment analysis of functional genes in the turquoise module. KB, blank group; FWA, Fuzi water-soluble alkaloids; FWD, Fuzi water decoction; KEGG, Kyoto encyclopedia of genes and genomes.

models of HF, with FWA showing greater efficacy.

Discussion

HF is the end stage of many cardiovascular diseases and the leading cause of death from heart diseases. In the course of HF, myocardial hypertrophy emerges as a major predisposing factor to its development.[22] Fuzi, a processed product derived from the daughter root of *Aconitum carmichaeli* Debx., finds widespread use in China and other Asian countries for treating various ailments, including HF and acute myocardial infarction. Here, we successfully constructed an *in vivo* HF model induced by propafenone hydrochloride and an *in vitro HDAC2* overexpression cardiac hypertrophy model using lentiviral transfection techniques. Previous studies from the group have demonstrated that different concentrations of FWD and FWA can inhibit the increase in left ventricular cardiomyocyte area, and reduce collagen volume fraction and cell apoptosis rate, thereby improving left ventricular function in rats with HF.[20,23] Therefore, based on transcriptome analysis, this study identified the main pathways involved in HF treatment by FWD and FWA as the PI3K-Akt signaling pathway, NF-kappa B signaling pathway, TNF signaling pathway, and ABC transporters. By analyzing WGCNA we clarified that ABC transporters might be the key pathway of Fuzi to improve HF.

At present, the establishment of HF models, both domestically and internationally, primarily relies on surgical and chemical drug-induced methods. For example, myocardial ischemia is simulated by increasing cardiac load through physical means such as aortic narrowing or coronary artery ligation, and in addition, the animals can be intervened by drugs, such as adriamycin, isoproterenol, and propafenone hydrochloride.[24] In this study, propafenone hydrochloride significantly decreased LV+dp/dt$_{max}$, LV-dp/dt$_{max}$, and heart rates in rats, suggesting alterations in myocardial systolic and diastolic functions. In addition, ANP, BNP, Ang-II, and ALD, as indicators for evaluating HF, were significantly elevated in the rat HF model. The FWD-treated group exhibited a tendency to reduce all the indexes in the HF rat model, with significant differences observed in LV+dp/dtmax, BNP, and ALD levels in the middle and high dose groups during the 20–60 m period of drug administration. Besides the mentioned animal models, HF cell models can also be prepared, which are typically induced by neurohumoral factors such as catecholamines and angiotensin.[25] In recent years, cell modeling based on lentiviral transfection has emerged as a novel and reliable method to more realistically imitate the disease

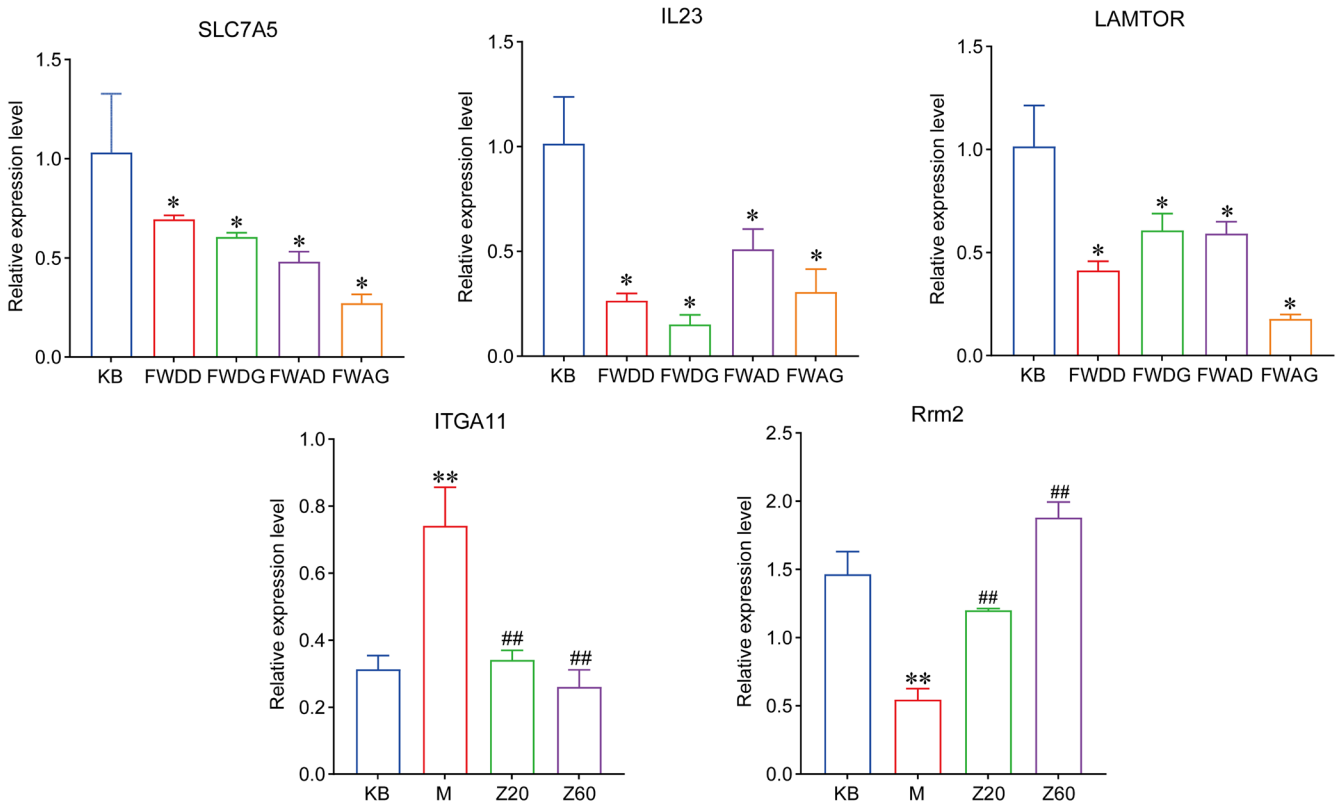

Fig. 6. qRT-PCR validation of differentially expressed genes (*$p < 0.05$, **$p < 0.01$ vs. the KB group; $^{\#\#}p < 0.01$ vs. the M group). FWAD, Fuzi water-soluble alkaloids - low dose; FWAG, Fuzi water-soluble alkaloids - high dose; FWDD, Fuzi water decoction - low dose; FWDG, Fuzi water decoction- high dose; KB, blank group; M, model group; qRT-PCR, quantitative real-time polymerase chain reaction; Z20, Administer Fuzi water decoction-mild dose for 20 minutes; Z60, Administer Fuzi water decoction-mild dose for 60 minutes.

process *in vitro*. This study further utilized lentiviral overexpression vectors to construct an in vitro model of cardiac hypertrophy with stable expression of exogenous *HDAC2*. The results showed an increase in cell surface area and an upregulation of *ANP*, *BNP*, *HDAC2* mRNA, and protein expression levels, indicating the successful establishment of an in vitro cardiomyocyte hypertrophy model.

HDAC2 belongs to the superfamily of class I HDACs, which induce cardiac hypertrophy when specifically overexpressed in the heart, and the cell model we constructed similarly exhibited hypertrophic features.[26] In the treated groups of FWD and FWA, we observed down-regulation of *HDAC2* and several regulatory genes. *HSP70* not only binds to *HDAC2* and co-induces cardiomyocyte hypertrophy but also participates in the disease process as a co-modulator of *HDAC2*.[27] mTOR is a key factor regulating cell growth in both physiological and pathological conditions of cardiac hypertrophy. Inhibitors of class I *HDACs* inhibit *mTOR* expression and ameliorate myocardial hypertrophy.[28] In this study, both FWD and FWA-treated groups exhibited down-regulation of *HSP70*, *HDAC2*, and *mTOR* expression, suggesting improved hypertrophy. It has been demonstrated that *HDAC2* is involved in the regulation of *CDKN1A*, and *HDAC2* is recruited by *FOXO3a* into the promoter of *CDKN1A* to regulate P21 expression in cerebellar granule neurons.[29,30] *CDKN1A* plays an important role in cell cycle progression, and the overexpression of *CDKN1A* can promote cell senescence, apoptosis, and hypertrophy of H9C2 cardiomyocytes.[31,32] Furthermore, genome-wide association and Mendelian randomization analyses suggest *CDKN1A* involvement in HF pathogenesis.[33] In this study, *CDKN1A* expression was significantly upregulated in the HF rat model, while it was downregulated after FWD administration. Similarly, downregulation of *CDKN1A* expression was also observed in the mast cell model treated with FWAG.

HF occurs through various mechanisms such as apoptosis, proliferation, inflammation, and calcium channel changes. Cardiac hypertrophy, as an important part of HF development, is regulated by cell growth, apoptosis, and mitochondrial energy metabolism. Based on transcriptomic analysis of *ex vivo* and *in vivo* HF models, the present study revealed that molecular mechanisms regulating myocardial hypertrophy and HF are associated with multiple pathways. In both *in vivo* and *ex vivo* models, differential genes were significantly enriched in the PI3K-Akt signaling pathway, NF-κB signaling pathway, and MAPK signaling pathway, which regulate cell proliferation, apoptosis, and inflammation. In addition, compared to the FWD-treated group, we observed significant enrichment of DEGs in the ABC transporter in the FWA-treated group. WGCNA results suggested that FWA ameliorates HF mainly through the ABC transporter and aminoacyl-tRNA biosynthetic pathways.

Mitochondrial dysfunction is widely acknowledged as a pivotal factor in HF progression. ABC transporters, a class of mitochondrial membrane transporter proteins, play a key role in the regulation of iron metabolism and the maintenance of cellular redox homeostasis, whereas iron imbalance and oxidative stress

are important factors in pathological changes such as cardiac hypertrophy and HF. Actually, a change in the source of ATP from fatty acid oxidation to glycolysis was observed during HF in humans and animal models.[34] Seventeen ABC transporters function in the human heart, including up-regulated differential genes *ABCB1*, *ABCB6*, *ABCB7*, *ABCB10*, and *ABCC8* obtained in this study. Among them, *ABCB7* and *ABCB8* are involved in cellular iron homeostasis and cytosolic iron-sulfur cluster biogenesis, and *ABCB10* participates in heme synthesis and iron metabolism; in addition, *ABCB10* protects cells from oxidative stress.[35] However, the Fe-S cluster and heme are cofactors in various biochemical pathways such as the tricarboxylic acid cycle and oxidative phosphorylation.[36,37] SLC7A5, a glutamine transporter protein, is upregulated during cardiac hypertrophy, promoting glutamine catabolism and uptake through significant aerobic glycolysis and glutamine degradation in hypertrophic cardiomyocytes.[38]

ECM serves as a crucial substrate in cardiac development; and integrins, primary receptors for ECM components, play a pivotal role in maintaining cardiovascular homeostasis. *ITGB1*, a member of the integrin family, activates the PI3K-Akt pathway, playing a protective role in apoptosis.[39] TLR2, involved in various cardiovascular diseases, not only induces an inflammatory response through activation of the NF-κB pathway, but also plays a role in myocardial hypertrophy.[40–43] TLR2 deficiency significantly ameliorates myocardial hypertrophy, fibrosis, and inflammation in rats. *TLR2* expression was down-regulated after 4 mg/mL FWA administration in this study, suggesting its benefit in alleviating cellular hypertrophy. C-myc, a proto-oncogene, participates in cell growth and apoptosis, associated with myocardial hypertrophy where the MAPK pathway plays an important role. Inhibiting the MAPK and downstream c-myc signaling pathways can exhibit anti-fibrosis and anti-myocardial hypertrophy effects in HF.[44] Protein kinase A (PKA) mediates various signaling pathways during myocardial hypertrophy, promoting PKA activation and downstream factor NFATc dephosphorylation to induce hypertrophic gene expression under hypertrophic stimuli. Among the DEGs, the expression levels of *PKA* and *NFATc* were downregulated. In addition, FWD and FWA can inhibit cardiomyocyte apoptosis by down-regulating *Caspase-3* and up-regulating *Bcl-2* expression.

Conclusions

Fuzi exhibits a certain inhibitory effect on the hypertrophic gene *HDAC2* and improves HF by regulating ABC transporters, the PI3K-Akt pathway, the NF-κB signaling pathway, and the cell cycle regulatory gene *CDKN1A*. FWA is essential for treating HF, and the expression of ABC transporter-related genes may regulate mitochondrial dysfunction effectively.

Acknowledgments

We thank the State Key Laboratory of Southwest Chinese Medicine Resources, Chengdu University of Traditional Chinese Medicine, for providing the decoction of FWD and FWA.

Funding

This work was supported by National Natural Science Foundation of China (81891010, 81891012), National Interdisciplinary Innovation Team of Traditional Chinese Medicine (ZYYCXTD-D-202209), Key project at central government level: The ability establishment of sustainable use for valuable Chinese medicine resources (2060302), School fund in Chengdu University of TCM (QJRC2022029), Science and technology research project of Sichuan Administration of Traditional Chinese Medicine (Study on the influence of traditional Chinese medicine for nourishing Yin and Quelling wind on clinical evaluation indexes and airway neurogenic inflammation in patients with chronic mild to moderate asthma, 2021MS169) and Chengdu major science and technology application demonstration project (Research and development and application demonstration of immersive Chinese intangible cultural heritage health care experience system, 2022-YF09-00058-SN).

Conflict of interest

The authors have no conflict of interests related to this publication.

Author contributions

Study concept and design (JHG, CP), acquisition of data (JZ, JHG), analysis and interpretation of data (JHG, FXH, JZ), drafting of the manuscript (JZ, DZ), administrative, technical, or material support (CP), and study supervision (XFX). All authors have made a significant contribution to this study and have approved the final manuscript.

Ethics statement

This study was carried out in accordance with the recommendations in the Guide for the Care and Use of Laboratory Animals of the National Institutes of Health. The protocol was approved by the Committee on the Ethics of Animal Experiments of Chengdu University of Traditional Chinese Medicine (Protocol Number: 2023020). All surgery was performed under sodium pentobarbital anesthesia, and all efforts were made to minimize suffering.

Data sharing statement

The dataset used in support of the findings of this study is available from the corresponding author at gaojihai@cdutcm.edu.cn upon request.

References

[1] Baman JR, Ahmad FS. Heart Failure. JAMA 2020;324(10):1015. doi:10.1001/jama.2020.13310, PMID:32749448.
[2] Deng B, Wang JX, Hu XX, Duan P, Wang L, Li Y, *et al*. Nkx2.5 enhances the efficacy of mesenchymal stem cells transplantation in treatment heart failure in rats. Life Sci 2017;182:65–72. doi:10.1016/j.lfs.2017.06.014, PMID:28624390.
[3] Nedkoff L, Weber C. Heart failure: not just a disease of the elderly. Heart 2022;108(4):249–250. doi:10.1136/heartjnl-2021-320273, PMID:34810240.
[4] Willerson JT. The Medical and Device-Related Treatment of Heart Failure. Circ Res 2019;124(11):1519. doi:10.1161/CIRCRESAHA.119.315268, PMID:31120816.
[5] Qi H, Ren J, E M, Zhang Q, Cao Y, Ba L, *et al*. MiR-103 inhibiting cardiac hypertrophy through inactivation of myocardial cell autophagy via targeting TRPV3 channel in rat hearts. J Cell Mol Med 2019;23(3):1926–1939. doi:10.1111/jcmm.14095, PMID:30604587.
[6] Trivedi CM, Luo Y, Yin Z, Zhang M, Zhu W, Wang T, *et al*. Hdac2 regulates the cardiac hypertrophic response by modulating Gsk3 beta activity. Nat Med 2007;13(3):324–331. doi:10.1038/nm1552, PMID:17322895.
[7] Zhang M, Yang X, Zimmerman RJ, Wang Q, Ross MA, Granger JM,

et al. CaMKII exacerbates heart failure progression by activating class I HDACs. J Mol Cell Cardiol 2020;149:73–81. doi:10.1016/j.yjmcc.2020.09.007, PMID:32971072.
[8] Chinese Pharmacopoeia Commission. Pharmacopoeia of the People's Republic of China 2020;BeijingThe Medicine Science and Technology Press of China.
[9] Tai CJ, El-Shazly M, Yang YH, Tsai YH, Csupor D, Hohmann J, *et al*. The effectiveness of Fuzi in combination with routine heart failure treatment on chronic heart failure patients. J Ethnopharmacol 2022;289:115040. doi:10.1016/j.jep.2022.115040, PMID:35121051.
[10] Li CJ, Zhai RR, Zhu XY, Guo ZF, Yang H. Discovery of effective combination from Renshen-Fuzi herbal pair against heart failure by spectrum-effect relationship analysis and zebrafish models. J Ethnopharmacol 2023;317:116832. doi:10.1016/j.jep.2023.116832, PMID:37352946.
[11] Shi L, Zhao Y, Feng C, Miao F, Dong L, Wang T, *et al*. Therapeutic effects of shaogan fuzi decoction in rheumatoid arthritis: Network pharmacology and experimental validation. Front Pharmacol 2022;13:967164. doi:10.3389/fphar.2022.967164, PMID:36059943.
[12] Zhao X, Yi Y, Jiang C, Huang X, Wen X, Liao H, *et al*. Gancao Fuzi decoction regulates the Th17/Treg cell imbalance in rheumatoid arthritis by targeting Foxp3 via miR-34a. J Ethnopharmacol 2023;301:115837. doi:10.1016/j.jep.2022.115837, PMID:36252875.
[13] Liu M, Li Y, Tang Y, Zheng L, Peng C. Synergistic effect of Aconiti Lateralis Radix Praeparata water-soluble alkaloids and Ginseng Radix et Rhizoma total ginsenosides compatibility on acute heart failure rats. J Chromatogr B Analyt Technol Biomed Life Sci 2020;1137:121935. doi:10.1016/j.jchromb.2019.121935, PMID:31877430.
[14] Zhang L, Lu X, Wang J, Li P, Li H, Wei S, *et al*. Zingiberis rhizoma mediated enhancement of the pharmacological effect of aconiti lateralis radix praeparata against acute heart failure and the underlying biological mechanisms. Biomed Pharmacother 2017;96:246–255. doi:10.1016/j.biopha.2017.09.145, PMID:28987949.
[15] Luo Z, Jiang M, Liu S, Duan Y, Huang J, Zeng H. Shenfu injection alleviates the clinical symptoms of heart failure patients combined with conventional treatment: A protocol for systematic review and meta-analysis of randomized clinical trials. Medicine (Baltimore) 2021;100(15):e23736. doi:10.1097/MD.0000000000023736, PMID:33847606.
[16] Zhang F, Zhang Y, Li X, Zhang S, Zhu M, Du W, *et al*. Research on Q-markers of Qiliqiangxin capsule for chronic heart failure treatment based on pharmacokinetics and pharmacodynamics association. Phytomedicine 2018;44:220–230. doi:10.1016/j.phymed.2018.03.003, PMID:29699844.
[17] Li G, Peng C, Xu X, Li J, Xie X. Cardiotonic effects of components from Lateralis Radix Praeparata on isolated rat hearts. Shi Zhen Guo Yi Guo Yao 2021;32(2):265–268. doi:10.3969/j.issn.1008-0805.2021.02.03.
[18] Xu X, Li G, Sun C, Chen J, Peng C, Xie X, *et al*. Research Progress on Water-Soluble Alkaloids from Fuzi and Their Pharmacological Effects. Pharmacology and Clinics of Chinese Materia Medica 2021;37(5):213–219. doi:10.13412/j.cnki.zyyl.2021.05.029.
[19] Hosseini A, Safari MK, Rajabian A, Boroumand-Noughabi S, Eid AH, Al Dhaheri Y, *et al*. Cardioprotective Effect of Rheum turkestanicum Against Doxorubicin-Induced Toxicity in Rats. Front Pharmacol 2022;13:909079. doi:10.3389/fphar.2022.909079, PMID:35754479.
[20] Xu X, Xie X, Zhang H, Wang P, Li G, Chen J, *et al*. Water-soluble alkaloids extracted from Aconiti Radix lateralis praeparata protect against chronic heart failure in rats via a calcium signaling pathway. Biomed Pharmacother 2021;135:111184. doi:10.1016/j.biopha.2020.111184, PMID:33418305.
[21] Yin Y, Xie X, Cao X, Li G, Chen J, Gao J, *et al*. Study on the molecular mechanism of Fuzi treating cardiac hypertrophy based on transcriptiomics and HDAC2-overexpression lentiviral vector. Pharmacy and Clinics of Chinese Materia Medica 2022;13(3):46–52.
[22] Shimizu I, Minamino T. Physiological and pathological cardiac hypertrophy. J Mol Cell Cardiol 2016;97:245–262. doi:10.1016/j.yjmcc.2016.06.001, PMID:27262674.
[23] Zhan H, Peng C. Effect of the compatibility with Radix Aconiti Lateralis Preparata and Rhizoma Zingiberis on adrephrin, angiotensinII, aldosterone, ANP and NT of blood plasma in Xinyang declination rats. Pharmacology and Clinics of Chinese Materia Medica 2006;22(2):12–14.
[24] Zhang Y, Chen W, Wang Y. STING is an essential regulator of heart inflammation and fibrosis in mice with pathological cardiac hypertrophy via endoplasmic reticulum (ER) stress. Biomed Pharmacother 2020;125:110022. doi:10.1016/j.biopha.2020.110022, PMID:32106379.
[25] Liu BY, Li L, Liu GL, Ding W, Chang WG, Xu T, *et al*. Baicalein attenuates cardiac hypertrophy in mice via suppressing oxidative stress and activating autophagy in cardiomyocytes. Acta Pharmacol Sin 2021;42(5):701–714. doi:10.1038/s41401-020-0496-1, PMID:32796955.
[26] Gao W, Ma X, Chen P, Zheng C. Research progress in the role and mechanism of class I and class II histone deacetylase for heart failure. Central South Pharmacy 2022;20(10):2329–2335. doi:10.7539/j.issn.1672-2981.2022.10.020.
[27] Kee HJ, Eom GH, Joung H, Shin S, Kim JR, Cho YK, *et al*. Activation of histone deacetylase 2 by inducible heat shock protein 70 in cardiac hypertrophy. Circ Res 2008;103(11):1259–1269. doi:10.1161/01.RES.0000338570.27156.84, PMID:18849323.
[28] Morales CR, Li DL, Pedrozo Z, May HI, Jiang N, Kyrychenko V, *et al*. Inhibition of class I histone deacetylases blunts cardiac hypertrophy through TSC2-dependent mTOR repression. Sci Signal 2016;9(422):ra34. doi:10.1126/scisignal.aad5736, PMID:27048565.
[29] Mattioli E, Andrenacci D, Garofalo C, Prencipe S, Scotlandi K, Remondini D, *et al*. Altered modulation of lamin A/C-HDAC2 interaction and p21 expression during oxidative stress response in HGPS. Aging Cell 2018;17(5):e12824. doi:10.1111/acel.12824, PMID:30109767.
[30] Peng S, Zhao S, Yan F, Cheng J, Huang L, Chen H, *et al*. HDAC2 selectively regulates FOXO3a-mediated gene transcription during oxidative stress-induced neuronal cell death. J Neurosci 2015;35(3):1250–1259. doi:10.1523/JNEUROSCI.2444-14.2015, PMID:25609639.
[31] Drozdkova DH, Gursky J, Minarik J, Überall I, Kolar Z, Trtkova KS. CDKN1A Gene Expression in Two Multiple Myeloma Cell Lines With Different P53 Functionality. Anticancer Res 2020;40(9):4979–4987. doi:10.21873/anticanres.14501, PMID:32878786.
[32] Mou H, Huang Z, Guo J. Study on the Mechanism of miR-499a-5p Targeting CDKN1A Gene in Cardiomyocyte Hypertrophy. Chinese Journal of Integrative Medicine on Cardio-Cerebrovascular Disease 2023;21(7):1218–1223. doi:10.12102/j.issn.1672-1349.2023.07.010.
[33] Shah S, Henry A, Roselli C, Lin H, Sveinbjörnsson G, Fatemifar G, *et al*. Genome-wide association and Mendelian randomisation analysis provide insights into the pathogenesis of heart failure. Nat Commun 2020;11(1):163. doi:10.1038/s41467-019-13690-5, PMID:31919418.
[34] Aubert G, Vega RB, Kelly DP. Perturbations in the gene regulatory pathways controlling mitochondrial energy production in the failing heart. Biochim Biophys Acta 2013;1833(4):840–847. doi:10.1016/j.bbamcr.2012.08.015, PMID:22964268.
[35] Thomas C, Tampé R. Structural and Mechanistic Principles of ABC Transporters. Annu Rev Biochem 2020;89:605–636. doi:10.1146/annurev-biochem-011520-105201, PMID:32569521.
[36] Schaedler TA, Faust B, Shintre CA, Carpenter EP, Srinivasan V, van Veen HW, *et al*. Structures and functions of mitochondrial ABC transporters. Biochem Soc Trans 2015;43(5):943–951. doi:10.1042/BST20150118, PMID:26517908.
[37] Zhabyeyev P, Oudit GY. Unravelling the molecular basis for cardiac iron metabolism and deficiency in heart failure. Eur Heart J 2017;38(5):373–375. doi:10.1093/eurheartj/ehw386, PMID:27651442.
[38] Piao L, Fang YH, Parikh K, Ryan JJ, Toth PT, Archer SL. Cardiac glutaminolysis: a maladaptive cancer metabolism pathway in the right ventricle in pulmonary hypertension. J Mol Med (Berl) 2013;91(10):1185–1197. doi:10.1007/s00109-013-1064-7, PMID:23794090.
[39] Menon B, Johnson JN, Ross RS, Singh M, Singh K. Glycogen synthase kinase-3beta plays a pro-apoptotic role in beta-adrenergic receptor-stimulated apoptosis in adult rat ventricular myocytes: Role of beta1 integrins. J Mol Cell Cardiol 2007;42(3):653–661. doi:10.1016/j.yjmcc.2006.12.011, PMID:17292911.
[40] Ferenčić A, Cuculić D, Stemberga V, Šešo B, Arbanas S, Jakovac H. Left ventricular hypertrophy is associated with overexpression of HSP60, TLR2, and TLR4 in the myocardium. Scand J Clin Lab Invest 2020;80(3):236–246. doi:10.1080/00365513.2020.1725977, PMID:32057259.
[41] Higashikuni Y, Tanaka K, Kato M, Nureki O, Hirata Y, Nagai R, *et al*.

Toll-like receptor-2 mediates adaptive cardiac hypertrophy in response to pressure overload through interleukin-1β upregulation via nuclear factor κB activation. J Am Heart Assoc 2013;2(6):e000267. doi:10.1161/JAHA.113.000267, PMID:24249711.

[42] Qian J, Liang S, Wang Q, Xu J, Huang W, Wu G, *et al*. Toll-like receptor-2 in cardiomyocytes and macrophages mediates isoproterenol-induced cardiac inflammation and remodeling. FASEB J 2023;37(2):e22740. doi:10.1096/fj.202201345R, PMID:36583707.

[43] Ye S, Lin K, Wu G, Xu MJ, Shan P, Huang W, *et al*. Toll-like receptor 2 signaling deficiency in cardiac cells ameliorates Ang II-induced cardiac inflammation and remodeling. Transl Res 2021;233:62–76. doi:10.1016/j.trsl.2021.02.011, PMID:33652137.

[44] Wang M, Luo W, Yu T, Liang S, Zou C, Sun J, *et al*. Diacerein alleviates Ang II-induced cardiac inflammation and remodeling by inhibiting the MAPKs/c-Myc pathway. Phytomedicine 2022;106:154387. doi:10.1016/j.phymed.2022.154387, PMID:36027716.